Atomic multiple-wave interferometer phase-shifted by the scalar Aharonov-Bohm effect

Takatoshi Aoki, Makoto Yasuhara, and Atsuo Morinaga
Faculty of Science and Technology, Tokyo University of Science, 2641 Yamazaki, Noda-shi, Chiba 278-8510, Japan
(Received 7 October 2002; published 15 May 2003)

A time-domain atomic multiple-wave interferometer using laser-cooled and trapped sodium atoms has been developed under pulsed magnetic fields. Each atomic phase was shifted due to the scalar Aharonov-Bohm effect by applying spatially homogeneous pulsed magnetic fields between numerous Raman excitation laser pulses. Interference fringes with a finesse of 11 were demonstrated for 11 successive Raman pulses and ten magnetic-field pulses.

DOI: 10.1103/PhysRevA.67.053602 PACS number(s): 03.75.Dg, 03.65.Vf, 39.20.+q, 32.80.Pj

I. INTRODUCTION

Nowadays, atomic interferometers are used as sensitive detectors for a variety of precise measurements, or they are used to test fundamental physics [1]. In particular, the Ramsey-Bordé atom interferometers comprised of separated laser fields [2,3] have become powerful and indispensable tools for precise measurements of gravitational acceleration [4], Planck constant mass ratio of h/m [5], and the rotation of the Earth [6]. Also, they are used for highly sensitive measurements of the Aharonov-Casher effect [7,8] and the scalar Aharonov-Bohm effect [9,10]. However, it is expected to develop an atomic multiple-wave interferometer such as a Fabry-Perot interferometer in the field of light optics. Because the sensitivity of the phase of the atomic N-wave interferometer is improved by a factor of $N/2$ compared with that of the two-wave interferometer.

The study of the atomic multiple-wave interferometer (hereafter referred to as AMI) was started by Ramsey using a thermal atomic beam with several spatially separated microwave fields [11]. However, the spatial and apparatus limitations limit the number of fields. On the other hand, recent laser-cooling technology has enabled fabrication of the time-domain atomic interferometer using cold atoms that are excited by numerous pulsed laser beams separated in time [9].

Currently, several kinds of AMIs have been developed using the cold atom. In the optical Ramsey geometry, Hinderthür *et al.* observed interference signals with a finesse of 140 for 160 successive light pulses [12]. On the other hand, the authors have developed a Ramsey-type AMI comprised of numerous copropagating stimulated Raman transitions and observed a finesse of 180 for 200 successive Raman pulses [13]. However, in the Ramsey resonance, the phase differences between the atomic waves are generated from the optical phase which is the detuning frequency multiplied by the time interval. The coherence of the Ramsey fringes is limited to the spectral width of the transit time.

Recently, atomic multiple-wave interferences with a real atomic phase shift caused by the scalar Aharonov-Bohm (SAB) effect during the time evolution of the atomic wave were reported. The first one was interferences between nine magnetic sublevels that have different phase shifts depending on their magnetic quantum number and on the strength of the time-dependent magnetic field [14]. The other one was a coherent superposition of the five ground-state Zeeman sublevels in a pulsed light shift potential [15]. They demonstrated sharply high-contrasted peaked fringes, however, the finesses of these interferometers are limited because of the finite number of the atomic internal states.

It should be noted that the coherence of the atomic wave that was shifted by the SAB effect is not limited because of its nondispersivity. In fact, the authors measured the SAB effect by applying a spatially homogeneous magnetic pulse between the two Raman pulses and were able to verify the nondispersivity of the SAB effect over a phase shift of more than 200 rad, which exceeds the coherent length by two orders of magnitude [10]. Therefore, in order to generate interference fringes sensitive to the magnetic field, the use of the Ramsey-type AMI and the SAB effect was attempted. In principle, the finesse of the interference fringes can be improved by increasing the number of Raman pulses. The important differences between the present AMI and the previous Ramsey-type AMI are the utilization of the magnetic-field-sensitive states and the application of spatially homogeneous magnetic-field pulses during numerous excitation pulses. Consequently, a residual time- and space-dependent magnetism must be removed since it washes out the interference signal.

In this paper, the principle of the atomic multiple-wave interferometer phase-shifted by the SAB effect and a demonstration of high-finesse interference signals by eliminating undesirable inhomogeneous magnetism are described.

II. PRINCIPLE

The principle and experimental procedure of our Ramsey-type AMI were described in detail in a previous paper [13]. Therefore, here is a short summary of the principle. Consider a two-level atom at rest, which interacts with numerous copropagating traveling laser pulses irradiating with the same time intervals, as shown in Fig. 1. It is assumed that the excitation amplitude of each laser beam is very weak. At every interaction, a partial wave packet of the excited state is produced from the main wave packet of the ground state. At the same time, the wave packet of the excited state obtains momentum in the propagation direction of the laser beams, but the momentum is assumed to be negligible in the case of rf Ramsey excitation. Consequently, the n-wave packets of the excited state interfere after n-pulse excitations. Using a geometrical analysis method [16], the population probability

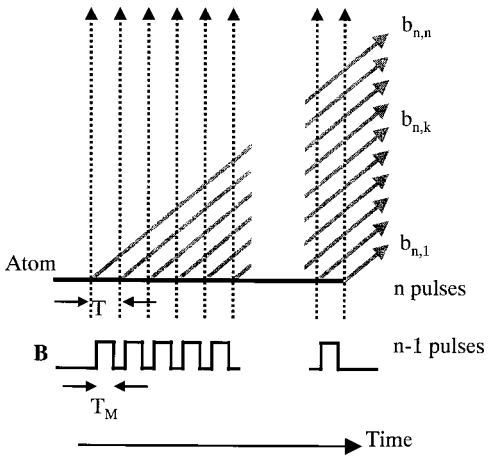

FIG. 1. Principle of the time-domain atomic multiple-wave interferometer phase-shifted by the scalar Aharonov-Bohm effect. The interferometer is composed of n laser pulses and $(n-1)$ magnetic-field pulses with a width T_M between adjacent laser pulses with an interval T. $b_{n,k}$ denotes the partially excited wave function splitted by the ith laser beam. The real splitting angles are close to zero for the copropagating Raman transitions used in this experiment.

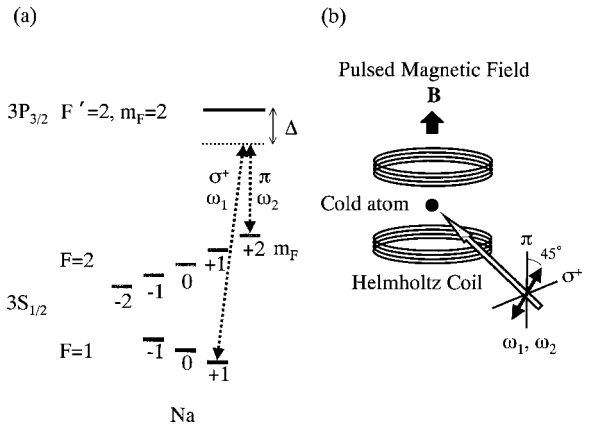

FIG. 2. (a) Zeeman splitting of the related hyperfine levels of sodium atoms under the magnetic field. (b) Experimental configuration. Cold atom ensemble is excited by a σ^+-polarized beam with a frequency, ω_1 and a π-polarized beam with a frequency ω_2 under the magnetic field.

of the excited state $b_n b_n^*$ after interaction with n pulses becomes

$$b_n b_n^* = \left(\sum_{k=1}^{n} b_{n,k} \right) \left(\sum_{k=1}^{n} b_{n,k}^* \right) \simeq \beta^2 \left[n + 2 \sum_{m=1}^{n-1} (n-m) \cos\{m(\Omega T + \Phi)\} \right], \quad (1)$$

where β is the small excitation amplitude, Ω is the detuning angular frequency, and Φ is the phase difference between the wave packets of the excited state and the ground state generated during T. In the case of $\Phi = 0$, the probability of the excited state oscillates as a function of the detuning of the laser frequency from the resonance frequency, which is known as a Ramsey fringe. With numerous laser beams, sharp interference fringes such as the Fabry-Perot interference occur as determined using Eq. (1). Actually, the demonstration of the interference fringes with a finesse of 180 for 200 successive excitation laser pulses was successful [13]. However, if the phase difference between the wave packets of the excited and ground states is changed by a perturbation, sharp interference fringes would be obtained as a function of the degree of perturbation.

The scalar Aharonov-Bohm effect shifts the phase of the atomic wave in the Zeeman sublevel under a time-dependent magnetic field [17]. The denotation of the ground state is $|F, m_F\rangle$ and that of the excited state is $|F', m_{F'}\rangle$, where F and F' are the quantum numbers of the total angular momentum, and m_F and $m_{F'}$ are the magnetic quantum numbers. When the magnetic field B is applied during a time duration T_M $(T_M < T)$, the phase shift between the two different states is given by

$$\Phi_{\mathrm{SAB}} = (g_{F'} m_{F'} - g_F m_F) \mu_B B T_M / \hbar, \quad (2)$$

where g_F is the Landé g factor and μ_B is the Bohr magneton. The authors have already confirmed the SAB effect using a time-domain atom interferometer comprised of two excitation laser pulses and a magnetic field applied between them [10]. Consequently, in order to obtain an atomic n-wave interference phase-shifted by the SAB effect in the present geometry, $n-1$ magnetic-field pulses with the same strength and the same pulse width must be applied during every adjacent laser pulses, as shown in Fig. 1. Then the sharp resonance profile such as an Airy's formula will be obtained as a function of Φ_{SAB}, which depends on the strength of the magnetic field B. In this method, the number of wave packets, which interferes with each other, depends on the number of excitation laser beams, thus it is not limited, in principle. The width of the multiple resonance is about twice that excited by two pulses with a separation of $(n-1)T$. This indicates that the sensitivity of the AMI to the strength of the magnetic field improved by a factor of $n/2$ compared with the two-pulse excitation for the same T_M.

In order to realize this AMI phase-shifted by the SAB effect, the two long-lived Zeeman ground hyperfine states of $F=1$ and $F=2$ of sodium atoms were used, which are coupled with copropagating two-photon Raman transitions. With a quantization axis of the magnetic field, two hyperfine levels are split in the Zeeman sublevels, as shown in Fig. 2(a). The largest phase shift due to the SAB effect is observed between the states of $|S_{1/2},1,1\rangle$ (which means $3S_{1/2}$, $F=1$, $M_F=1$) and $|S_{1/2},2,2\rangle$, which are selected by a couple of σ^+-polarized transitions of $|S_{1/2},1,1\rangle$ to $|P_{3/2},2,2\rangle$ and the π-polarized transition of $|S_{1/2},2,2\rangle$ to $|P_{3/2},2,2\rangle$. Their frequencies are ω_1 and ω_2, respectively. Then the phase shift is represented by $\Phi_{\mathrm{SAB}} = 3/2 \mu_B B T_M / \hbar$ from Eq. (2).

III. EXPERIMENTAL

A. Experimental procedure

The experimental apparatuses used were almost the same as those described before [13], except for the apparatus for

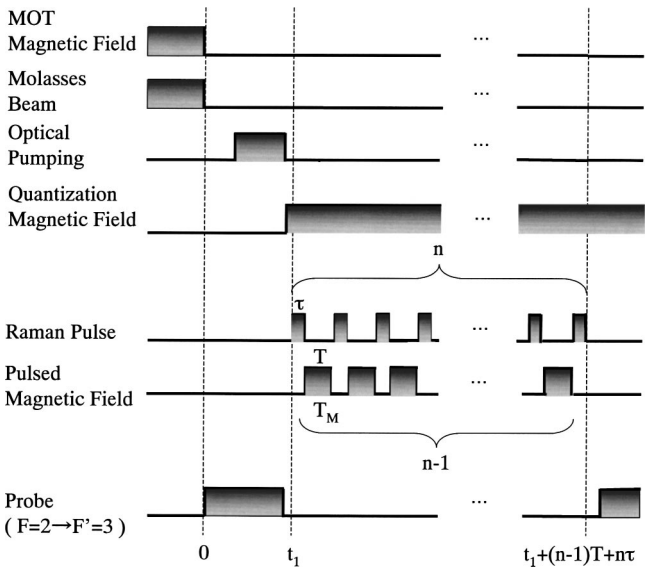

FIG. 3. Timing diagram of the experimental procedure.

the magnetic field generation. The cold sodium atomic ensemble was prepared as follows. First, the sodium atomic beam from the oven was slowed down to the velocity of 50 m/s by the circular polarizing counterpropagating laser beam using the Zeeman cooling technique. The stable laser beam was generated from a dye laser system stabilized to iodine molecules using FM spectroscopy [18]. Then the slowed down atomic beam reached the glass cell (trap region) and atoms were trapped by three pairs of counterpropagating laser beams orthogonal to each other at the center of the magneto-optical trap (MOT). The density of the trapped atoms was 5×10^{10} cm^{-3} and the number of atoms was 1×10^{9}. The trap conditions will be reported in more detail in another paper [19].

The time sequence diagram after the MOT is shown in Fig. 3. After the trap loading time of 2 s, the quadrupole magnetic field was turned off and then the atoms were cooled to 200 μK by polarization gradient cooling for 3 ms. After that, all molasses laser beams were turned off and the probe laser beam was turned on. The probe laser beam that was tuned to the transition from the $|S_{1/2},2\rangle$ to $|P_{3/2},3\rangle$ states was used in order to monitor the population in the $|S_{1/2},2\rangle$ state. The transmittance of the probe beam T_1 was measured to determine the number of atoms in the $|S_{1/2},2\rangle$ state during 50 μs. All atoms in the $|S_{1/2},2\rangle$ state were optically pumped to the $|S_{1/2},1\rangle$ state via the $P_{3/2}$ state. After the optical pumping for 300 μs, all laser beams were turned off.

In order to construct the AMI, the two-photon Raman transitions between the states of $|S_{1/2},1,1\rangle$ and $|S_{1/2},2,2\rangle$ via $|P_{3/2},2,2\rangle$ were used, as shown in Fig. 2(b). A magnetic field was applied to the cold ensemble to define the quantization axis. Next, the stimulated Raman transition laser beams with frequencies of ω_1 and ω_2 were used as beam splitters for the atom interferometer. The frequencies ω_1 and ω_2 were red-detuned about 500 MHz from the transitions $|S_{1/2},1\rangle$ to $|P_{3/2},2\rangle$ and $|S_{1/2},2\rangle$ to $|P_{3/2},2\rangle$, respectively. Then the spontaneous emission from the $3P_{3/2}$ state became negligibly small for a large detuning frequency of 500 MHz. Therefore, the $|S_{1/2},1\rangle$ and $|S_{1/2},2\rangle$ states can be treated as a two-level system. Carrier and high sideband frequencies produced by an electro-optic modulator were used as the frequencies ω_1 and ω_2 for the two-photon transitions. The power of the carrier frequency was set to be equal to that of the sideband frequency. The sideband frequency of about 1.772 GHz was tuned to the resonance frequency of the transition from $|S_{1/2},1,1\rangle$ to $|S_{1/2},2,2\rangle$, under the quantized magnetic field.

To select the Zeeman state, the Raman beams were propagated perpendicular to the quantization axis (z axis) with a linear polarization at an angle of 45° from the z axis, which was decomposed to σ^+ and π polarizations. Numerous amounts of Raman pulses were applied to the cold atoms, and a sequence of the homogeneous magnetic-field pulse B parallel to the quantization axis due to the second Helmholtz coil was applied between adjacent Raman beam pulses. A typical pulse width of the Raman beam τ was 3 μs, a separation time T between the two adjacent Raman pulses was 13 μs, and the pulse width T_M of the homogeneous magnetic field was 5 μs.

Finally, the probe beam was turned on and transmittance T_2 was measured. From the ratio of T_1 to T_2, the excitation probability of the transition from $|S_{1/2},1\rangle$ to $|S_{1/2},2\rangle$ by the successive Raman pulses was obtained. The excitation probability was monitored as a function of the magnetic field B. The above time sequence was repeated every 10 ms and the excitation probabilities for each of the runs were accumulated and averaged in a computer.

B. Visibility of Ramsey resonance

The atom interferometer based on the magnetic sublevels is affected by residual magnetic fields, thus the visibility of the interference decreases easily. The cold sample in our experiment had a diameter of 3 mm. For spatial inhomogeneous magnetic field, the Ramsey phase of ΩT in Eq. (1) depends on the location of the atom, thus the interference fringes are washed out after the summation of all the atoms. On the other hand, a time-dependent magnetic field shifts the resonance frequency of the atom as a function of time, thus the coherence of the atom is also disturbed. Therefore, a reduction of the spatial and temporal inhomogeneity of the background magnetic field, as well as its magnitude is necessary.

The constant background magnetic field was determined to be less than 30 mG using three pairs of Helmholtz coils arranged along three orthogonal directions. Then the quantization magnetic field was applied. The main inhomogeneous magnetic field was generated from the Zeeman coil to slow down the atom. The leakage of the magnetic field at the trap region was 7 mG/mm in the direction of the atomic beam axis. To eliminate leakage of the magnetic field, an anti-Helmholtz coil was used that yielded a strong gradient magnetic field along the atomic beam axis and a zero field at the center of the trap. Figure 4 shows the visibility of the Ramsey resonance versus the current of the anti-Helmholtz coil. At a current of 1 A, the maximum visibility was obtained. The typical signal of the Ramsey fringes with magnetic sensitive states is shown in Fig. 5, which was measured using

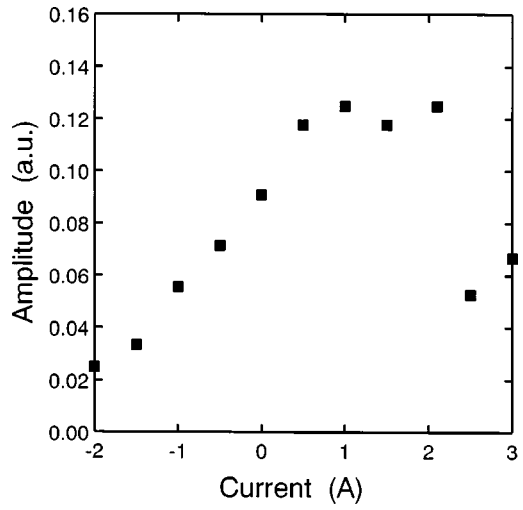

FIG. 4. Amplitude of the Ramsey fringe versus the current of the anti-Helmholtz coil used in compensation for the spatial inhomogeneous magnetic field.

two Raman beam pulses with a pulse width of 20 μs and a pulse interval of 60 μs.

To avoid the eddy current induced in the metal vacuum chamber after the magnetic field was turned off, a glass cell was used. The temporal variation in the magnetic field occurred after quadrupole magnetic fields for MOT were turned off. The time constant for turning it off was about 100 μs. The residual field decreased to 3 mG/mm at 300 μs after turning off. Therefore, the quadrupole magnetic field for MOT could be removed almost completely at 3 ms after turning off. The amplitude of the Ramsey resonance with the optimized current of the anti-Helmholtz coil after 3 ms was measured as a function of the separation time between the two Raman pulses, as shown in Fig. 6. As the separation time increased, the visibility decreased with a time constant of 320 μs. This result indicates that the residual spatial inhomogeneous magnetic field was about 1 mG/mm. In the case of the 0-0 transition between the $|S_{1/2},1,0\rangle$ and $|S_{1/2},2,0\rangle$ states, the time constant was more than 2 ms because these states have only the second-order Zeeman energy effect.

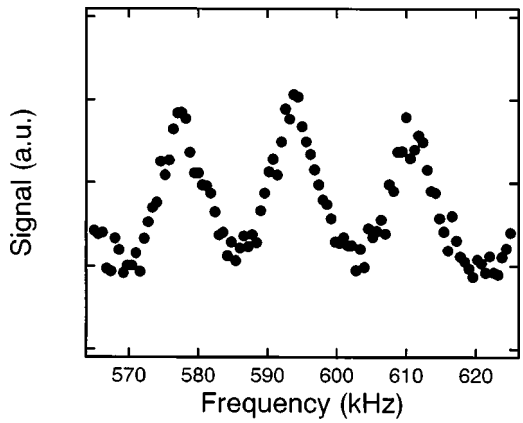

FIG. 5. Typical Ramsey fringes with two Raman laser beams under the magnetic field.

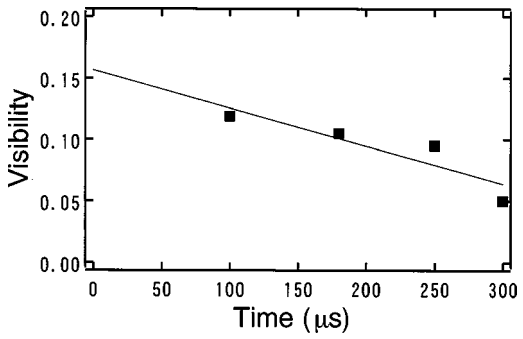

FIG. 6. Visibility as a function of the separation time between the two Raman laser pulses, which were measured at 3 ms after the magnetic field of MOT was turned off.

C. Calibration of pulsed magnetic field

In order to calibrate the magnetic-field strength, the Zeeman frequency shift of the multiple Ramsey resonance under the magnetic field was measured. In this experiment, a constant magnetic field was applied to the cold ensemble during the time from the first to the last Raman pulses. The frequency shift of the Ramsey resonance was measured for the current applied to the Helmholtz coil. Figure 7 shows the typical signal of AMI with 11 Raman pulses in the transition between the $|S_{1/2},1,1\rangle$ and $|S_{1/2},2,2\rangle$ states. The pulse width of Raman beam τ was 3 μs and the separation time T between the two pulses was 13 μs. The width of the enveloped curve was the reciprocal of the interaction time of 3 μs, the free spectral range (FSR) was the reciprocal of the separation time of 13 μs and the resonance width was the reciprocal of the separation time between the first and last pulses of 160 μs.

The Zeeman frequency shift was observed from the result of the multiple Ramsey resonance with a finesse of 11 for various applied currents as shown in Fig. 8. Using these results, the absolute value of the magnetic field against the applied current was calibrated to be $B/I=0.9365 \pm 0.0001$ mG/mA.

IV. RESULTS AND DISCUSSION

First, the dependence of the interference signal on the excitation power of the Raman beam was examined for the AMI with four successive laser pulses and three pulses of the SAB magnetic field parallel to the quantization axis in inter-

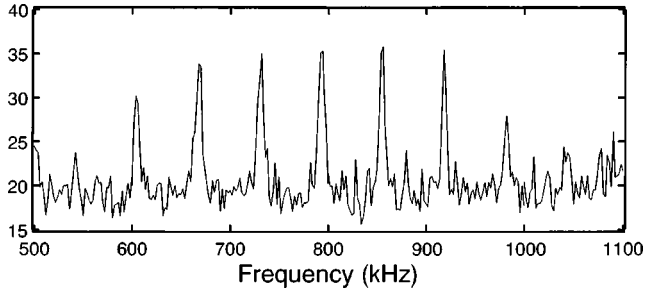

FIG. 7. Typical Ramsey fringes with 11 Raman laser pulses under the magnetic field.

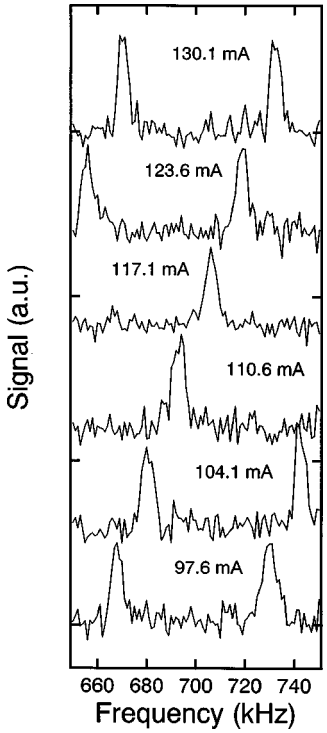

FIG. 8. Zeeman frequency shift of the Ramsey resonance with 11 Raman laser pulses for various magnetic-field strengths.

vals between adjacent pulses. The pulse width of the Raman beams was 5 μs and the pulse interval was 35 μs. T_M was 20 μs. Figure 9 shows the interference signals as a function of the strength of the SAB field for various excitation powers of the Raman beams. It is clearly observed that the pattern of the fringes changes markedly depending on the excitation power. Using the geometrical analysis, the interference signal can be calculated by [13]

$$b_4 b_4^* = (4\alpha^6\beta^2 - 8\alpha^4\beta^4 + 8\alpha^2\beta^6) + 2(3\alpha^6\beta^2 - 8\alpha^4\beta^4 + 4\alpha^2\beta^6)\cos(\Phi_{\mathrm{SAB}}) + 2(2\alpha^6\beta^2 - 4\alpha^4\beta^4) \times \cos(2\Phi_{\mathrm{SAB}}) + 2(\alpha^6\beta^2)\cos(3\Phi_{\mathrm{SAB}}). \quad (3)$$

The calculated signals are also given in Fig. 9 by dashed curves and they well describe the behavior of the experimental results. With the further decrease of the excitation power of the Raman beams, Eq. (3) was reduced to Eq. (1). The Ramsey resonance with a finesse of four and suppressed sidelobes was obtained as shown in Fig. 10, where the pulse width of the Raman beams was 10 μs, pulse interval was 50 μs, and T_M was 30 μs. The power of one component of a Raman laser beam was 7 mW, which corresponds to $\beta = 0.13$. The integration number at each point was 6.

Finally, the principle of AMI phase-shifted by the SAB effect was demonstrated with a finesse of 11. The 11 Raman laser pulses with a pulse width of 3 μs and a pulse interval of 13 μs were applied to the cold atom. A power of one component of the Raman laser beam corresponds to $\beta = 0.03$. The ten magnetic pulses with a width T_M of 5 μs were applied between every adjacent Raman pulses. The integration number at each point was 15 and the interference signal as a function of the strength of the SAB magnetic fields is shown in Fig. 11. The full width at half maximum was 10.4 mG and the FSR was 111.0 mG, which corresponds to the finesse of 11. If the present coherent time is improved to more than 1 ms, it will be possible to apply 100 Raman pulses with a pulse interval of 10 μs and 99 magnetic-field pulses with a width of 5 μs. Then sharp interference fringes with a width of 1 mG will be obtained.

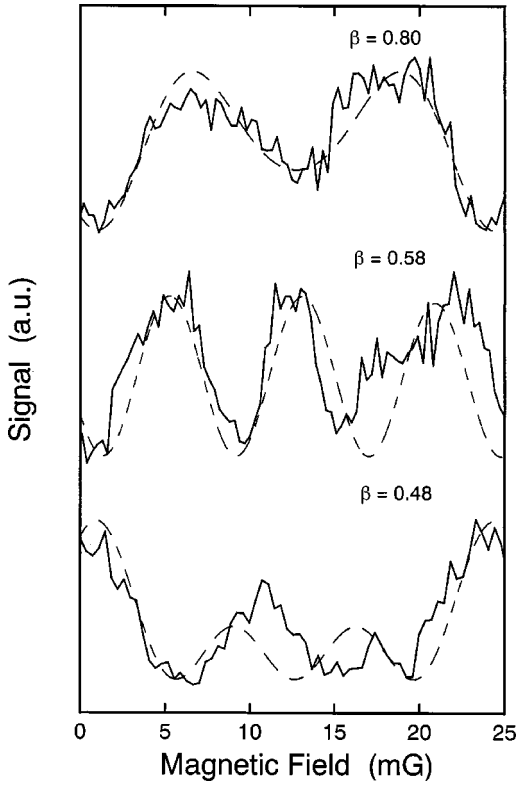

FIG. 9. Interference signal with four Raman laser pulses and three pulsed magnetic field versus the strength of magnetic field for different excitation amplitudes β. The experimental results (solid line) are compared with the calculated results (dashed line).

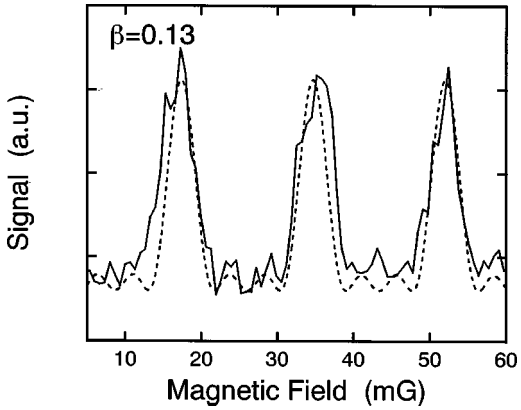

FIG. 10. Typical interference signal of the atomic four-wave interferometer phase-shifted by the scalar Aharonov-Bohm effect.

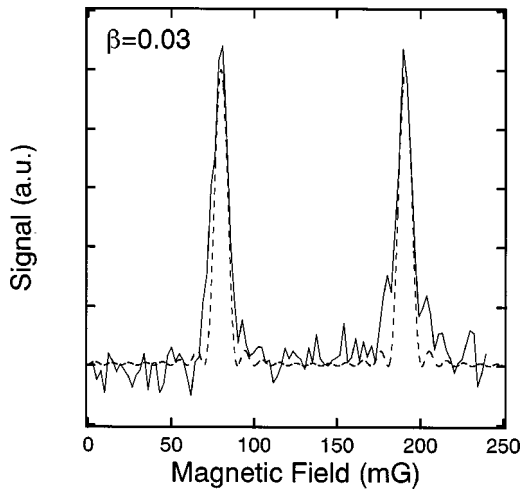

FIG. 11. Typical interference signal of the atomic multiple-wave interferometer phase-shifted by the scalar Aharonov-Bohm effect. The cold atom ensemble was excited by 11 Raman laser pulses and was applied by ten magnetic-field pulses between adjacent laser beams.

V. CONCLUSION

The demonstration of the multiple atomic interference fringes with a finesse of 11 using 11 Raman pulses and ten magnetic pulses during every adjacent Raman pulse was successful. The finesse obtained is the highest finesse in the AMI, which was obtained by shifting the phase of the atomic wave directly. If the residual spatial and temporal inhomogeneous magnetic field is eliminated completely, a finesse of more than 100 could be obtained as shown in the Ramsey-type AMI [13]. The final limit will be determined by a free fall due to the gravity of the cold atoms from the interaction zone. The benefits of this multipulse scheme are that one can get rid of additional sidelobes and smaller laser powers for the pulses can be used. Another benefit is that the coherence length of the atomic wave shifted by the SAB effect is not limited because of its nondispersivity. Thus, this interferometer can be useful in obtaining the sensitive measurement of the strength of the magnetic field for a large dynamic range.

The high-finesse atom interferometer will become a powerful and indispensable tool in obtaining precise physical measurements in the near future, similar to the optical Fabry-Perot interferometer.

ACKNOWLEDGMENTS

The authors would like to thank K. Shinohara for his contribution to the initial stage of this experiment. This research was supported in part by a Grant-in-Aid for Scientific Research on Priority Area (B) and for Encouragement of Young Scientists (B) of the Ministry of Education, Culture, Sports, Science and Technology (Japan).

[1] See, e.g., *Atom Interferometry*, edited by P. Berman (Academic Press, San Diego, 1997).
[2] C. J. Bordé, Phys. Lett. A **140**, 10 (1989).
[3] F. Riehle, Th. Kisters, A. Witte, J. Helmcke, and C. J. Borde, Phys. Rev. Lett. **67**, 177 (1991).
[4] M. Kasevich and S. Chu, Appl. Phys. B: Photophys. Laser Chem. **B54**, 321 (1992).
[5] D. S. Weiss, B. C. Young, and S. Chu, Phys. Rev. Lett. **70**, 2706 (1993).
[6] T. L. Gustavson, P. Bouyer, and M. A. Kasevich, Phys. Rev. Lett. **78**, 2046 (1997).
[7] K. Zeiske, G. Zinner, F. Riehle, and J. Helmcke, Appl. Phys. B: Lasers Opt. **B60**, 205 (1995).
[8] S. Yanagimachi, M. Kajiro, M. Machiya, and A. Morinaga, Phys. Rev. A **65**, 042104 (2002).
[9] J. H. Müller, D. Bettermann, V. Rieger, K. Sengstock, U. Sterr, and W. Ertmer, Appl. Phys. B: Lasers Opt. **B60**, 199 (1995).
[10] K. Shinohara, T. Aoki, and A. Morinaga, Phys. Rev. A **66**, 042106 (2002). In this paper, page 1, 5 lines before Eq. (1), V should be $V=m_F g_F \mu_B B(t)$ and in Eqs. (1) and (2), the first sign of "-" should be removed.
[11] N. F. Ramsey, Phys. Rev. **109**, 822 (1958).
[12] H. Hinderthür, F. Ruschewitz, H.-J. Lohe, S. Lechte, K. Sengstock, and W. Ertmer, Phys. Rev. A **59**, 2216 (1999).
[13] T. Aoki, K. Shinohara, and A. Morinaga, Phys. Rev. A **63**, 063611 (2001).
[14] É. Maréchal, R. Long, J.-L. Bossennec, R. Barbé, J.-C. Keller, and O. Gorceix, Phys. Rev. A **60**, 3197 (1999).
[15] M. Mei, T. W. Hänsch, and M. Weitz, Phys. Rev. A **61**, 020101(R) (2000).
[16] A. Morinaga, S. Yanagimachi, and T. Aoki, in *Proceedings of the 6th Symposium on Frequency Standard and Metrology*, edited by P. Gill (World Scientific, London, 2002), pp. 288–294.
[17] S. NicChormaic, Ch. Miniatura, O. Gorceix, B. V. Lesengo, J. Robert, S. Feron, V. Leorent, J. Reinhardt, J. Baudon, and K. Rubin, Phys. Rev. Lett. **72**, 1 (1994).
[18] S. Watanabe, Y. Aizawa, and A. Morinaga, Jpn. J. Appl. Phys., Part 1 **42**, 1462 (2003).
[19] S. Hayakawa, T. Aoki, R. Tajima, T. Miyaharu, M. Abe, and A. Morinaga (unpublished).